Detecting Adversarial Examples in Deep Neural Networks using Normalizing Filters

Shuangchi Gu[1], Ping Yi[1], Ting Zhu[2], Yao Yao[2] and Wei Wang[2]
[1]*School of Cyber Security, Shanghai Jiao Tong University, 800 Dongchuan Road, Shanghai, China*
[2]*Department of Computer Science and Electrical Engineering, University of Maryland Baltimore County, Baltimore, U.S.A.*

Keywords: Normalizing Filter, Adversarial Example, Detection Framework.

Abstract: Deep neural networks are vulnerable to *adversarial examples* which are inputs modified with unnoticeable but malicious perturbations. Most defending methods only focus on tuning the DNN itself, but we propose a novel defending method which modifies the input data to detect the adversarial examples. We establish a detection framework based on *normalizing filters* that can partially erase those perturbations by smoothing the input image or depth reduction work. The framework gives the decision by comparing the classification results of original input and multiple normalized inputs. Using several combinations of gaussian blur filter, median blur filter and depth reduction filter, the evaluation results reaches a high detection rate and achieves partial restoration work of adversarial examples in MNIST dataset. The whole detection framework is a low-cost highly extensible strategy in DNN defending works.

1 INTRODUCTION

Deep learning technology is being widely used in many industry fields, and Deep Neural Networks perform especially well on some artificial intelligence tasks. For instance, researchers use DNNs to classify images, sounds, and texts. In some specific situations like security applications, the robustness of the DNNs is important. However, recent studies have shown that DNN attackers can modify some images to misdirect the Deep Learning classification models, forcing them to misclassify those images. The maliciously generated images or other inputs are called adversarial examples (Goodfellow et al., 2014).

Adversarial examples are normally crafted by some specific attack algorithms. The hackers use such algorithms to add small but effective perturbations to contaminate the legitimate examples. The perturbations are generally invisible to human eyes, but the DNNs are susceptible to them. Basically, the existence of adversarial examples exposes the blind spots in the DNNs' training procedure.

The main goal of our work is to strengthen Deep Neural Networks against the adversarial examples. A pre-input framework is established to detect the adversarial examples and transform some of those images to normal ones. The ability of detecting adversarial examples is significant because even some state-of-the-art DNN models are vulnerable to adversarial attacks (Goodfellow et al., 2014), which means that some DNN classifiers deployed online are hopeless against those threats. That situation could be changed with deploying a detecting method for the input of DNNs.

Many previous works to strengthen the DNNs have made some achievements. For instance, adversarial training (Tramèr et al., 2017a) uses a large number of adversarial examples to retrain the DNN model. It mainly focuses on modifying the model itself, and the model would be able to defend one specific attack after training with adversarial examples crafted by that. Like adversarial training, many previous defensive works could not defend several attack simultaneously, and cost a lot.

In a CNN classification system, the input is normally an 8bit grey image or a 24bit color image, which means that the feature space of the input is unnecessarily large. The training data is only a minor part of the feature space, and the rest of the input feature space will provide extensive probability for the existence of adversarial examples. On the other hand, the adversarial perturbations are mostly a minor modification on the legitimate image, so the distance between the legitimate and adversarial images are relatively small. If some normalizing image filters are applied to the adversarial examples, the nega-

Gu, S., Yi, P., Zhu, T., Yao, Y. and Wang, W.
Detecting Adversarial Examples in Deep Neural Networks using Normalizing Filters.
DOI: 10.5220/0007370301640173
In *Proceedings of the 11th International Conference on Agents and Artificial Intelligence (ICAART 2019)*, pages 164-173
ISBN: 978-989-758-350-6

tive effects of adversarial perturbations may be easily erased. Based on that facts, the major contribution of this paper is as follow.

- Low-cost filters based on *normalizing* algorithms which can decrease the effect of adversarial perturbations are applied to the input images.
- We raised a novel *normalized prediction inconsistency* algorithm which use the prediction vectors to detect the adversarial examples.
- The pre-input framework based on normalizing filters appears to be an effective and a less expensive way to enhance the robustness of DNN models in our evaluation.

The paper is structured as follows. Section 2 introduces basic technology about adversarial examples and some previous work to defend adversarial attacks. Several normalizing filters are presented in section 3 and will be evaluated with the framework in section 4.

2 BACKGROUND AND RELATED WORKS

This section provides a concise introduction to adversarial examples generating methods and normal defensive methods.

2.1 Adversarial Examples Generating Methods

An adversarial example is an input which is able to mislead the target classifier but is not sensitive to human perception. It is crafted from a legitimate example by an adversary with a limited perturbation.

Adversarial examples can be *targeted*, the legitimate example x would be classified as a particular class by adversarial perturbation, formally, using a given $x \in X$ and classify function $f(\cdot)$, the goal of a targeted adversarial attack with target $\alpha \in A$ is to find an $x' \in X$ that

$$f(x') = \alpha \wedge \triangle(x, x') \leq \varepsilon \quad (1)$$

the $\triangle$ presents the distance between x and x'. Furthermore, adversarial examples can be *untargeted*, in which case the adversary's goal is just for x' to be classified as any class other than its correct class, which is

$$f(x') \neq f(x) \wedge \triangle(x, x') \leq \varepsilon \quad (2)$$

The perturbation intensity ε is the limit of image modifications. The smaller it is, the more similar the adversarial and legitimate examples are. In other words, the adversarial example seems to be "legitimate" to a human observer. In equation (1) and (2), the distance function $\triangle(x, x')$ is basically a L_p-*norm* metric.

2.1.1 Fast Gradient Sign Method

Goodfellow et al. (Goodfellow et al., 2014) proposed the *fast gradient sign method* (FGSM) to find the adversarial examples effectively. The perturbation is calculated directly by using gradient vector of the loss function $J(\cdot, \cdot, \cdot)$ for training the target classifier:

$$\eta = \varepsilon sign(\nabla_x J(\theta, x, f(x))) \quad (3)$$

The adversarial examples processed by FGSM are untargeted, and the perturbations are calculated using the L_∞-norm.

2.1.2 Basic Iterative Method

Kurakin et al. (Kurakin et al., 2016) raised the *basic iterative method* (BIM) which is based on FGSM. The adversarial applies FGSM multiple times with small steps. For the original input x, the image at k iteration is

$$x'_k = x'_{k-1} + Clip_{x,\varepsilon}(\alpha \cdot sign(\nabla_x J(g(x'_{k-1}), y))) \quad (4)$$

The average distance between the legitimate and adversarial examples in BIM method is smaller than FGSM, which means the perturbations are harder to detect by human perception.

2.1.3 Jacobian Saliency Map Approach

Jacobian saliency map approach (JSMA) is proposed by Papernot et al. (Papernot et al., 2016c) which is a targeted method with the perturbations limited by L_0-norm, so this attack only modify a limited pixels of the original image. JSMA iteratively perturbs pixels in an input image that have high adversarial saliency scores. The adversarial saliency score of each pixel is calculated to reflect how this pixel will increase prediction probability of the target class α in the classifier model while decrease the probability of all other possible classes.

2.1.4 Carlini & Wagner Attack Method

Carlini et al. (Carlini and Wagner, 2017) recently introduced a gradient-based attack which can generate adversarial examples based on $L_0, L2, L_\infty$-norms, and it is more effective and stronger than other methods introduced above.

The C&W attack will be the key generating method in the evaluation section.

2.2 Defensive Methods against Adversaries

The defensive methods could be divided into two themes: model modification and data modification. The former methods include *adversarial training*, *gradient masking* (Papernot et al., 2016b) and others which mainly focus on the optimization of the CNN models. **Adversarial training** uses the adversarial examples and their corresponding ground truth labels as extra training data, thus the classifier would learn how to avoid the negative influence of the adversarial perturbations and become more robust ideally. **Gradient masking** aims to reduce the sensitivity of the classifiers to minor changes in input images. (Papernot et al., 2015) introduced a defensive distillation strategy to hide the gradient information from an adversary. But it was proved being vulnerable to black-box attack. The input normalizing framework proposed by us is a part of data modification, it keeps the CNN models unchanged and uses different normalizing filters to erase the minor perturbations.

As for detection, (Ma et al., 2018) raised a detection method using **local intrinsic dimensionality** (LID). The LID values of adversarial and legitimate examples are different so that the system can detect the adversarial examples if the LID value is abnormal. Ping et al. (YI Ping and Jianhua, 2018) surveyed the adversarial attacks in artificial intelligence.

3 NORMALIZING FILTERS & DETECTION METHOD

The **system structure** of the whole framework is shown in Fig. 1. In our work, we mainly focus on filters which are able to decrease the redundant information in the input images. After sufficient evaluation on numbers of different digital filters, two types of filters are deployed in *Normalizing Filters Pack* as our "normalizing filters": Gaussian & median blur filter and depth reduction filter, and the predictions of images using different filters would be sent into the judge module in Fig. 1, a proper algorithm based on *prediction inconsistency* is applied to the module.

The framework has high flexibility. The CNN classifier in the framework is replaceable. For each classifier, a specific configuration would be set to fit the input image type and format. The filters and the detection algorithm for different prediction vectors are also adjustable. Furthermore, the cost on the whole system is relatively low, the requirements for a long period of time and high-performance computation hardware is unnecessary.

3.1 Gaussian & Median Blur Filter

Blur filters are commonly used in daily situations to reduce noise or hide some particular information, which may be effective to "normalize" the perturbations. Here we describe the two types of blur algorithms.

3.1.1 Gaussian Blur Filter

The Gaussian blur filter uses a Gaussian function to calculate the transformation to apply to each pixel in the input image. With the standard deviation of the Gaussian distribution σ set, a convolutional matrix with dimensions $\lceil 6\sigma \rceil \times \lceil 6\sigma \rceil$ will be applied to the original image (*pixels at a distance of more than 3*σ *have almost-zero influence*). Applying a Gaussian filter with a proper deviation to an image does not mean to lose key information in the original image, but can partially remove the abruptly sharp pixels and edges, which can be the consequences of adversarial perturbations.

3.1.2 Median Blur Filter

The median blur filter's theory is a resemblant of Gaussian filter in image processing territory. The main idea of the median filter is to run through the original image pixel by pixel, replacing each pixel with the median of neighboring ones. The filter creates a "slide window" which slides over the entire image and finally output a smoothed image. The median blur filter actually makes adjacent pixels more similar and the slide window size is set according to different adversarial attack types. For instance, a relatively small value for window size will work on adversarial perturbations calculated through L_0-norm.

3.2 Depth Reduction Filter

Bit depth implies how redundant an image is in the color or greyscale aspect. For most images in usual cases, there would be some redundancy which means the observer can reduce the bit depth while keeps the key information in the original images. For instance, a grayscale image in MNIST (LeCun et al., 1990) provides $2^8 = 256$ possible values for each pixel, but the image actually keeps its information using 1-bit depth filter. Thus, a depth reduction filter would not evidently influence the target CNN classifier's performance.

For some attacks based on L_∞-norm, the adversarial perturbations appears to be fuzzy patterns, which

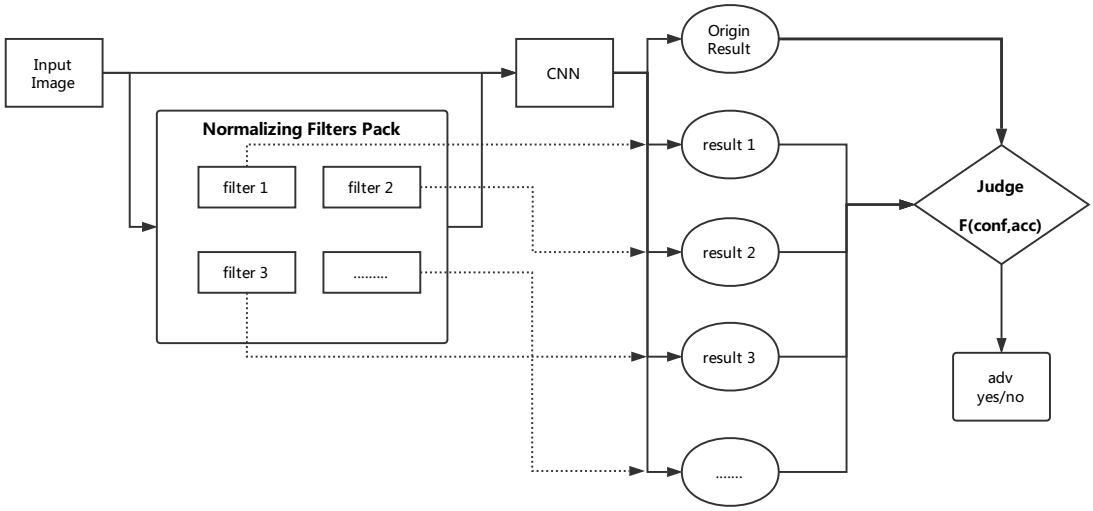

Figure 1: The Adversarial Examples Detection Framework. The CNN receives both original image and images modified by normalizing filters, then the predictions are sent into judge module to figure out whether the original image is an adversarial.

Figure 2: Gaussian & median blur filters at multiple configurations. Both filters are effective to reduce abruptly-occurring pixels in this case.

indicates the color space of that image is too big to generate a specific perturbation. Thus the adversarial perturbations may be cleared if the color space is reduced. On the other hand, the bit depth should not be too small if the image is relatively complicated, the effect of different depth is shown in Fig. 3.

3.3 Implementations of Filters

The Gaussian and median blur filters we used in the evaluation section are implemented in the *Scipy module* (Jones et al., 2014). The median filter will be set with a 2×2 slide window in low resolution datasets and an additional 3×3 window in ImageNet (Krizhevsky et al., 2012). case. As for Gaussian filters, different value of σ from 0.5 to 2.0 will be tested in all datasets. Fig. 2 are living instance for both filters.

The formula below is adopted to simulate the depth reduction filters. Variable *ogdep* and *dep* indicate the bit depth of the original image (8 in the chosen datasets) and the aim (1 to 7).

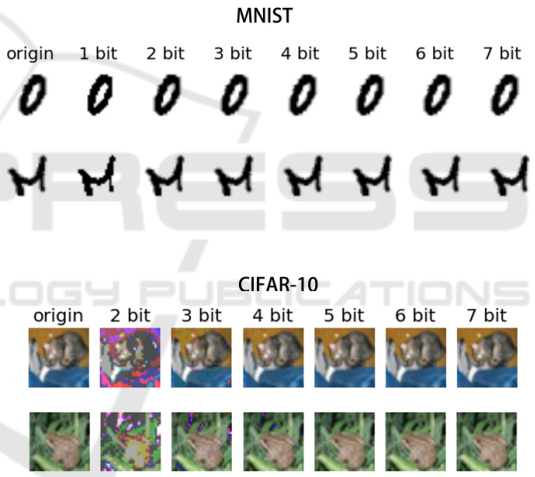

Figure 3: Depth Reduction Filters at different settings: as shown in the MNIST dataset, the images still keep the key information, but situations are totally opposite in the CIFAR-10 dataset (Krizhevsky et al., 2014). As a result, the depth reduction filter chosen in the final defensive framework should be specified by the target CNN classifier.

$$rec = \left\lfloor \frac{\left\lfloor \frac{img}{2^{ogdep}-1} \times 2^{dep}-1 \right\rfloor \times 2^{ogdep}-1}{2^{dep}-1} \right\rfloor \quad (5)$$

3.4 Detection Methods

The basic method of detecting adversarial examples is named *prediction inconsistency* (Hinton et al., 2012). It means one adversarial example will have different predictions using several classifiers which have the

same function.

However, (Tramèr et al., 2017b) have proved the transferability of the adversarial examples even the adversarial space, thus we raised a novel concept of prediction inconsistency: *normalized prediction inconsistency*. This method is based on the predictions of the same image in several normalizing filters using the same classifier. Because of the normalizing filters we use have little influence on legitimate examples, images which have the prediction inconsistency issues are likely to be adversarial examples.

The methods to measure the distance between predictions is flexible. A prediction generated by the target classifier is represented as a vector of probability distributions, thus, we can compare the vectors of probability distributions using L_1, L_2-norms, or training a *support vector machine* to detect the normalized prediction inconsistency phenomenon. We finally choose L_2-norm-based distance to judge the difference in the evaluation section.

$$dist_2^{(og,\,nmlzd)} = \left\| f(x)_{og} - f(x)_{nmlzd} \right\|_2, \quad f(x) = \langle p_1(x),\, p_2(x), \cdots, p_k(x) \rangle \tag{6}$$

Here $f(x)_{og}$ indicates the prediction vector of original input image, and $f(x)_{nmlzd}$ is that of the image "normalized" by one of the filters. Each prediction vector should contain 5 to 10 probabilities in general conditions.

Last but not the least, it is not enough to get the distances between several prediction vectors, the algorithm for calculating the inconsistency level and a standard threshold value is significant for estimate the comprehensive result whether the original input image is adversarial. We noticed that different filters have significantly different influence on the same adversarial attack algorithm, so the larger the distance is, the more important it could be.

$$fin_2^{(k,dist)} = \frac{1}{n}\sum_i dist_i^k, \;\; k = 1,2,3,\cdots \tag{7}$$

The parameter k here implies the importance of outstandingly large distances, as k became bigger, the value of $dist_i^k$ would tend to be zero if $dist_i$ is relatively small, like distances in a legitimate example's case. Here parameter k would be 2 in our evaluation.

The normalizing filters and detecting methods finally just work together as Fig. 1.

4 EVALUATION OF NORMALIZING FILTERS

After introduction about adversarial examples, normalizing filters and detecting methods towards adversaries. We have arrived at some primary conclusion and requirements:

- Many images used in the classification task contain redundant and irrelevant information.
- Normalizing filters are designed to ignore the redundancy of the input images.
- Normalizing filters should be able to destroy the influence of adversarial perturbation.
- Normalizing filters should not impact the accuracy of the target CNN classifiers.

Next step is to evaluate whether normalizing filters could satisfy those requirements. In the next section, the detecting methods will be tested combined with filters.

4.1 Experiment Setup

The image classifiers we use are mentioned above: Maxout Network (Goodfellow et al., 2013) for MNIST provided by *cleverhans* (Papernot et al., 2016a), DenseNet (Iandola et al., 2014) and Inception-V3. The accuracy of the classifiers are shown in Table 1.

Table 1: Statistics of Target CNN Classifiers.

Dataset & Classifier	Top-1 Acc	Top-5 Acc
MNIST Maxout Net	99.55%	/
CIFAR-10 DenseNet	95.12%	/
ILSVRC 12 Inception	78.8%	94.36%

The experiment contains up to seven attacks, including targeted (CW @L_0, CW @L_2) and untargeted attacks (FGSM, BIM, JSMA, CW @L_0, CW @L_2), all of the implementations are provided by the cleverhans lib (Papernot et al., 2016a). The hardware in the experiment includes an Intel Xeon E5-2680 v3 CPU, 128GB DDR 4 ECC memory and an NVIDIA Tesla M40 graphics card. For each dataset, we randomly choose 500 legitimate images for each adversarial attack, and we also adjust the parameters properly to generate 1000 adversarial examples for each type of attacks which have relatively high attack success rate over 90% and short distance ($L_0, L_2, L_\infty - norm$) according to the attack types, which is a guarantee for a proper attack strength. The CW attack (Carlini and

Wagner, 2017) could always generates adversarial examples with better attack success rate, and smaller perturbations, but it just takes 10× more time to generate the perturbation.

As for targeted attacks, we used the *least likely* class as the target, which has the smallest probability in the prediction vector. Thus we have covered almost all types of attacks in the evaluation.

4.2 Results on Normalizing Filters

The defence results are shown in Table 2 and some are figured in Fig. 4. All of the seven attacks above have been evaluated with three different datasets, and three normalizing filters are tested with eight configurations.

Gaussian & Median Blur Filters. In theory, blur algorithm would be effective to perturbations as abruptly sharp pixels and edges because it basically makes the pixels closer to their neighbors.

- **MNIST.** The gaussian and median filters both have two configurations on MNIST datasets. Both filters are relatively well performing against JSMA and CW @L_0 attacks, which is close to our hypothesis. As for the configurations, Gaussian filters perform slightly better at $\sigma = 0.6$ than $\sigma = 0.4$, and median filters perform worse at a 2×2 slide window than a 3×3 one. The effect of both filters on MNIST images are quite close, and the performance are similar too. It is noteworthy that the blur filters have minor impact on the accuracy of legitimate examples, which is partially because the information of MNIST images is quite simple and clear (just from 1 to 10).
- **CIFAR-10.** CIFAR-10 is basically a low resolution color image dataset, which means the images look like "blurred". So the configuration should be set with discretion. The σ value of gaussian filter is set to 0.3 which is lower than that on MNIST images, the median filter just use the smallest 2×2 slide window. For the results, the performance is relatively satisfying on L_0-norm attacks which is close to the results on MNIST dataset. The median filters work outstandingly well against JSMA attacks, that may be a coincidence because the limitation test batch size.
- **ImageNet.** The test results is slightly different on ImageNet dataset. Firstly, we discover that both filters have ordinary performance against FGSM and BIM attacks which increase the classifying accuracy up to 34.4%, it is an acceptable result for L_∞-norm attacks. Next, the performance on CW L_0 and L_2 attacks are close (69.8% 81.2% by median filter and 58.8% 70.6% by gaussian filter), that means the perturbation generated by CW attack can be roughly erased by blur algorithms. Actually, the truth is the perturbations of CW attack are less sensitive to human perception, but those tiny adjustment would be easily removed or confused.

According to the statistics in the last column of Table 2, the average confidence of normalized adversarial examples (processed by gaussian and median filters) decreases sharply, from about 90% to 60% in MNIST and CIFAR-10, and from 80% to 50% in ImageNet. That kind of decrease could be a signal of *prediction inconsistency* phenomenon, which will be discussed later.

Depth Reduction Filter. The major effect for depth reduction filter is reducing the rebundancy in images. The configuration of this filter varies in three datasets. In MNIST, the depth is reduced to 1-bit, which means it is actually a binary filter.In CIFAR-10 and ImageNet, we use two configurations: 5-bit and 6-bit to avoid losing the image's major information.

- **MNIST.** The binary filter works properly against L_∞ attacks. It boosts the accuracy to almost 100.0%, which is the same as legitimate examples'. The reason is obvious: the pixels in perturbations calculated with L_∞-norm are converted to either 0 (white) or 1 (black), and in order to be invisible to human eyes, the value of each pixel is always less than 0.5. The binary filter also outperforms other defence strategy in Fig. 5 As for CW @L_2 attack, the accuracy is still good at about 77.8%, but the binary filter seems to be in vain against CW @L_0 attack.
- **CIFAR-10.** Results on 5-bit and 6-bit are negative. The prediction accuracy of normalized image hardly reaches 30%, only the accuracy of CW @L_2 attack cases reaches 48.2%, which still is not a good result. The main reason of these results comes from the format of the images, which is 32×32 24-bit color image, the resolution of each sample is too low even human have to concentrate to recognize it. Thus, we believe that the depth reduction filter just simply ruins the image itself but the perturbations.
- **ImageNet.** Depth reduction filter works unsatisfying against $L_\infty and L_0$ attacks on ImageNet either. But the accuracy about L_2 attacks increases to 56.4% (untargeted) and 50.3% (targeted). Like what we have conclude above, the CW @L_2 attack generates almost invisible perturbations which can be easily influenced by other filters.

We have evaluated the performance of three filters

Table 2: Defence Statistics of Normalizing Filters: *Pm.* indicates the parameter of each filter, *OAcc.* is the accuracy of legitimate examples using normalizing filters and *Conf.* is the average prediction confidence of normalized adversarial examples.

Type	**Dataset**	**Pm.**	**OAcc.**	**Accuracy Under Attacks**							**Conf.**
				FGSM	BIM	JSMA	CW_0	CW_2	CW_{0T}	CW_{2T}	
Gaussian Filter	MNIST	0.4	99.2%	56.2%	28.6%	70.0%	50.2%	51.4%	/	/	60.5%
		0.6	98.5%	49.8%	19.4%	**80.8%**	60.3%	66.8%	/	/	68.3%
	CIFAR-10	0.3	88.3%	13.2%	15.2%	50.6%	**70.6%**	66.4%	68.8%	**69.6%**	72.1%
	ImageNet	0.4	64.1%	34.4%	32.3%	/	65.4%	58.8%	64.6%	59.0%	56.7%
		0.6	62.8%	33.2%	29.8%	/	**70.6%**	69.0%	66.6%	68.9%	60.6%
Median Filter	MNIST	2x2	99.3%	**60.2%**	34.5%	70.2%	63.3%	43.2%	/	/	67.3%
		3x3	99.0%	53.2%	20.3%	79.3%	60.4%	42.4%	/	/	64.3%
	CIFAR-10	2x2	90.4%	40.4%	14.6%	**90.8%**	70.4%	56.2%	**76.3%**	60.2%	55.2%
	ImageNet	2x2	66.5%	32.4%	33.2%	/	69.8%	70.5%	**81.2%**	75.6%	50.3%
		3x3	64.9%	32.8%	29.3%	/	**80.3%**	68.4%	76.8%	**79.0%**	45.5%
Depth Reduction	MNIST	1bit	99.3%	**100%**	**99.2%**	55.5%	5.4%	**77.8%**	/	/	93.8%
	CIFAR-10	6bit	92.1%	20.8%	13.7%	12.4%	6.2%	39.1%	0.8%	48.2%	53.5%
		5bit	93.4%	16.3%	10.6%	9.2%	10.1%	29.8%	1.6%	40.3%	46.1%
	ImageNet	6bit	68.2%	9.8%	8.8%	/	45.6%	56.4%	43.4%	50.3%	47.2%
		5bit	70.4%	1.2%	0.2%	/	22.1%	48.1%	19.8%	38.2%	43.5%

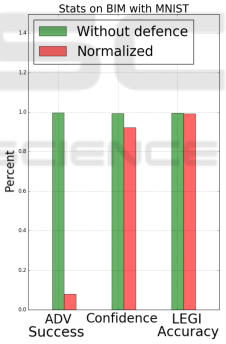

(a) Bit Depth @1bit

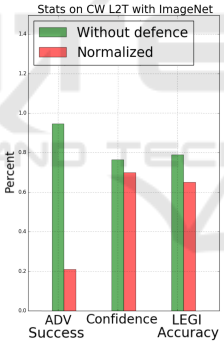

(b) Median 3×3

Figure 4: Part of the normalizing results on three datasets. The normalizing filters are effective to reduce the attack strength while barely influence the accuracy on legitimate examples.

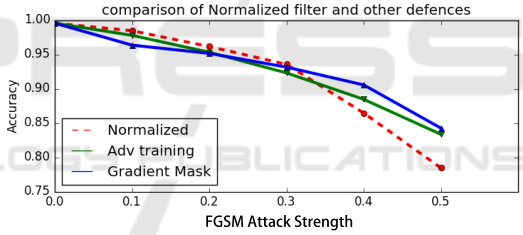

Figure 5: The binary filters perform well comparing with other defence methods. Here is the binary filter on MNIST against FGSM at different attack strength, the binary filter outperform the adversarial training and gradient masking at a relatively low strength ε.

so far. From the results in Table 2, it is obvious that those filters are not strong enough to use as a standalone defensive methods. However, some filters are able to erase a specific type of perturbations and others can reduce the confidence of adversarial examples, in other words, the normalizing filters can either destroy the perturbation or weaken it. Those features are the headspring of the idea to develop a detection framework using normalizing filters.

5 EVALUATION OF DETECTION FRAMEWORK

The confidence data of section 4 has been collected to analyze whether those adversarial examples have *normalized prediction inconsistency* issues. Using equation (7), the $fin_2^{(2,dist)}$ values of both legitimate and adversarial examples are shown in Fig. 6.

In Fig.6(a), most legitimate examples have no prediction inconsistency issues, the peak is around 0, and the situation is identical in Fig 6(b) with the peak about 0.1. On the other hand adversarial examples have an opposite circumstance, the peak is about 0.7 in MNIST and 0.6 in ImageNet.

Table 3: Statistics of Detection Framework: The MNIST dataset has the best results for its high detection rate and low false negative rate; Both CIFAR-10 and ImageNet are tested with two thresholds for either high detection rate or relatively low FNR.

Dataset	Configurations	Thresholds	Attacks	Detection Rate	FNR
MNIST	DRF 1-bit Median 2x2	0.04	L_∞	97.43%	0.13%
			L_2	98.20%	0%
			L_0	95.61%	0.18%
CIFAR	Median 2x2	0.221	L_∞	43.27%	1.42%
			L_2	78.33%	1.04%
			L_0	89.80%	0.41%
		0.473	L_∞	28.72%	0.55%
			L_2	66.07%	0.61%
			L_0	74.48%	0.39%
ImageNet	Gaussian 0.6 Median 3x3 DRF 5-bit	0.342	L_∞	80.21%	0.52%
			L_2	90.1%	0.41%
			L_0	86.34%	0.42%
		0.423	L_∞	77.54%	0.31%
			L_2	87.2%	0.33%
			L_0	84.32%	0.35%

Table 4: Comparison of the normalizing framework and the LID detecting method. The statistics are based on the result on MNIST.

Methods	Detect Rate	FNR	Cost	Adaptability
Normalizing Framework	97.08%	0.10%	Low	High
LID	97.56%	0.13%	Relatively High	Medium

5.1 Detection Threshold

A detection threshold value for $fin_2^{(2,dist)}$ in equation (7) should be set. The threshold value would be picked between two peaks in Fig. 6, and all images that have higher $fin_2^{(2,dist)}$ value would be considered as adversarial examples.

According to the results in Table 2, different groups of normalizing filters are tested for the three datasets, in MNIST, 1-bit depth reduction filter and median filter with a 2×2 core are chosen in the detection framework; we only use a median filter with a 2×2 core to normalize the CIFAR-10 images because other filters have unsatisfying results; for ImageNet, a gaussian filter with σ=0.6, a median filter with a 3×3 core, and a 5-bit depth reduction filter are chosen for the test.

Table 3 represents the test results of thresholds, which have been evaluated based on detection rate and false negative rate (FNR). We use both 10,000 adversarial and legitimate images for testing each configuration, and 1000 images for $CW@L_2$ attacks of ImageNet, which takes too much time.

- **MNIST.** Using 1-bit detph reduction filter and median filter with 2×2 core, the detection framework has a remarkable result on overall detection rate of 97.08%, the score on L_0, L_2, L_∞-norm attacks are all satisfying with an acceptable false negative rate at 0.103%. A lower threshold value would have minor influence the detection rate while significantly increase the false negative rate.

- **CIFAR-10.** Due to the unstable result on the normalizing filters, there is only one filter used in the CIFAR-10's detection framework. The biggest problem for other filters is the destructive modifications made to legitimate examples, which causes the false negative rate unacceptable. The results of the one-filter detection framework is not bad. The detection rate for $L_0 and L_2$ attacks reaches 78.33% and 89.80% with FNR at less than 1.10%. Although the detection rate of L_∞ attacks are 43.27%, the legitimate examples are hardly misjudged. A higher threshold at 0.473 can reduce the FNR to about 0.5%, but the detection rate falls nearly 13.5%.

- **ImageNet.** Detection rate with threshold at 0.342 and 0.423 is both good with average scores at

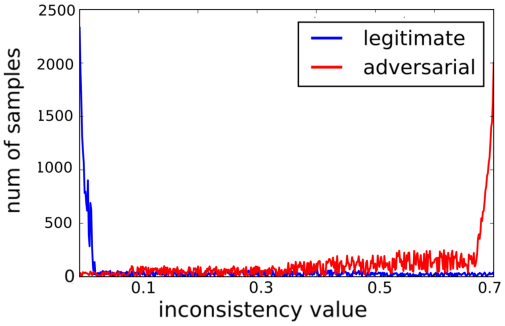

(a) MNIST inconsistency

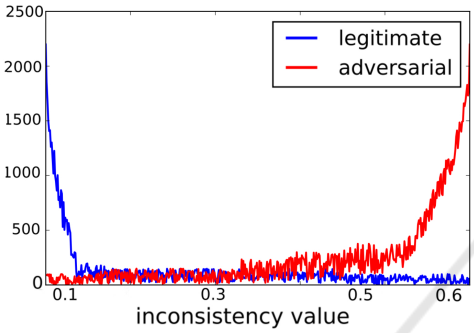

(b) ImageNet inconsistency

Figure 6: The difference of *prediction inconsistency* phenomenon between legitimate and adversarial examples, the score is based on L_2 distance of the predictions of normalized images and has a range from 0 to 1 in theory, but it is almost impossible to reach the 1 value because the prediction just varies after using the normalizing filters. The MNIST case uses a binary filter and the ImageNet case uses a median filter.

85.55% and 83.02%. But the difference in FNR is attention-getting, the 0.423 threshold performs way better than 0.342, especially in L_∞ attacks. We suppose that is an accidental event in picking test data.

Table 4 indicates the difference between the normalizing detection framework and LID-based method on MNIST dataset. We can conclude that the detection rate and false negative rate are close, but for the cost and adaptability of different CNN classifiers, the normalizing detection framework performs better, which is the main superiority. The LID method need to analyze the inner structure of the neural network and calculate the score at a deep layer of the classifier to ensure the best performance, its adaptability is not so good as the normalizing detection framework.

5.2 Restore Threshold

It is noticable that normalizing filters have impressive performance in the **MNIST** dataset, and due to adversarial perturbation is relatively unnoticeable (small), most adversarial examples could be "normalized" back to its original class, in other words, they could be restored. Thus, a restore threshold could be set to judge whether the prediction of adversarial example after normalizing is the original class.

$$\begin{aligned} class_{restore} &= \langle class_p,\ pred_p \rangle, \\ pred_p &= max(\ pred_1,\ pred_2, \cdots), \\ pred_i &\geq th_{restore} \end{aligned} \tag{8}$$

The restored class is calculated as equation (8), here $th_{restore}$ is the restore threshold value. In the prediction vector, only probabilities over the threshold would be considered as a candidate. The test for restore threshold value is in Table 5. As the data indicates, higher threshold means better accuracy of restoring, but fewer adversarial examples can be restored, for instance, the accuracy at 0.9 threshold is about 98.4% with a restored ratio at just 43.3%, but the restore ratio at 0.750 threshold can reach 80.8% with a lower restore accuracy.

Table 5: Restore Threshold and Restore Ratio for MNIST: the input images are adversarial examples detected by our detection framework. The threshold value is actually a restriction of confidence.

Env	Threshold	Accuracy	RR
MNIST with Detection	0.900	98.4%	43.3%
	0.880	96.7%	56.2%
	0.750	86.3%	80.8%

6 CONCLUSION

It is impressive that the normalizing filters can affect the adversarial examples, the detection and restore framework based on that also have alright effectiveness. What can not be ignored is the low cost of those normalizing filters, those filters use common algorithms which have relatively low pressure to the computation hardware. Comparing with adversarial training (Tramèr et al., 2017a), the detection framework could be used instantly rather than spending a long time training adversarial examples.

However, there are still some shortage in our general detection framework, the type of normalizing filters are limited, which can be vulnerable when detecting more complicated adversarial examples. Last but not the least, the detection method can be improved, it may be better to use a machine-learning-based technology, for example, *suppert vector machine* (Hearst et al., 1998), to make the decision.

The detection framework based on normalizing filters opens a different research direction of defend-

ing adversarial attacks, it is basically an add-on to the deep neural networks so that it can collaborate with other defence like adversarial training and gradient masking (Papernot et al., 2016b). We will focus on this type of defence to make it applicable in real-world scenes.

ACKNOWLEDGEMENTS

This work is supported by the National Natural Science Foundation of China(61571290, 61831007, 61431008), National Key Research and Development Program of China (2017YFB0802900, 2017YFB0802300, 2018YFB0803503), Shanghai Municipal Science and Technology Project under grant (16511102605, 16DZ1200702), NSF grants 1652669 and 1539047.

REFERENCES

Carlini, N. and Wagner, D. (2017). Towards evaluating the robustness of neural networks. In *Security and Privacy (SP), 2017 IEEE Symposium on*, pages 39–57. IEEE.

Goodfellow, I. J., Shlens, J., and Szegedy, C. (2014). Explaining and harnessing adversarial examples. *arXiv preprint arXiv:1412.6572*.

Goodfellow, I. J., Warde-Farley, D., Mirza, M., Courville, A., and Bengio, Y. (2013). Maxout networks. *arXiv preprint arXiv:1302.4389*.

Hearst, M. A., Dumais, S. T., Osuna, E., Platt, J., and Scholkopf, B. (1998). Support vector machines. *IEEE Intelligent Systems and their applications*, 13(4):18–28.

Hinton, G. E., Srivastava, N., Krizhevsky, A., Sutskever, I., and Salakhutdinov, R. R. (2012). Improving neural networks by preventing co-adaptation of feature detectors. *arXiv preprint arXiv:1207.0580*.

Iandola, F., Moskewicz, M., Karayev, S., Girshick, R., Darrell, T., and Keutzer, K. (2014). Densenet: Implementing efficient convnet descriptor pyramids. *arXiv preprint arXiv:1404.1869*.

Jones, E., Oliphant, T., and Peterson, P. (2014). {SciPy}: open source scientific tools for {Python}.

Krizhevsky, A., Nair, V., and Hinton, G. (2014). The cifar-10 dataset. *online: http://www. cs. toronto. edu/kriz/cifar. html*.

Krizhevsky, A., Sutskever, I., and Hinton, G. E. (2012). Imagenet classification with deep convolutional neural networks. In *Advances in neural information processing systems*, pages 1097–1105.

Kurakin, A., Goodfellow, I., and Bengio, S. (2016). Adversarial examples in the physical world. *arXiv preprint arXiv:1607.02533*.

LeCun, Y., Boser, B. E., Denker, J. S., Henderson, D., Howard, R. E., Hubbard, W. E., and Jackel, L. D. (1990). Handwritten digit recognition with a back-propagation network. In *Advances in neural information processing systems*, pages 396–404.

Ma, X., Li, B., Wang, Y., Erfani, S. M., Wijewickrema, S., Houle, M. E., Schoenebeck, G., Song, D., and Bailey, J. (2018). Characterizing adversarial subspaces using local intrinsic dimensionality. *arXiv preprint arXiv:1801.02613*.

Papernot, N., Carlini, N., Goodfellow, I., Feinman, R., Faghri, F., Matyasko, A., Hambardzumyan, K., Juang, Y.-L., Kurakin, A., Sheatsley, R., et al. (2016a). cleverhans v2. 0.0: an adversarial machine learning library. *arXiv preprint arXiv:1610.00768*.

Papernot, N., McDaniel, P., Goodfellow, I., Jha, S., Celik, Z. B., and Swami, A. (2016b). Practical black-box attacks against deep learning systems using adversarial examples. *arXiv preprint*.

Papernot, N., McDaniel, P., Jha, S., Fredrikson, M., Celik, Z. B., and Swami, A. (2016c). The limitations of deep learning in adversarial settings. In *Security and Privacy (EuroS&P), 2016 IEEE European Symposium on*, pages 372–387. IEEE.

Papernot, N., McDaniel, P., Wu, X., Jha, S., and Swami, A. (2015). Distillation as a defense to adversarial perturbations against deep neural networks. *arXiv preprint arXiv:1511.04508*.

Tramèr, F., Kurakin, A., Papernot, N., Goodfellow, I., Boneh, D., and McDaniel, P. (2017a). Ensemble adversarial training: Attacks and defenses. *arXiv preprint arXiv:1705.07204*.

Tramèr, F., Papernot, N., Goodfellow, I., Boneh, D., and McDaniel, P. (2017b). The space of transferable adversarial examples. *arXiv preprint arXiv:1704.03453*.

YI Ping, WANG Kedi, H. C. G. S. Z. F. and Jianhua, L. (2018). Adversarial attacks in artificial intelligence: A survey. *Journal of Shanhai Jiao Tong University*, 52(10):1298–1306.